

Contents lists available at ScienceDirect

Physics Letters B

www.elsevier.com/locate/physletb

Multi-hadron final states in RPV supersymmetric models with extra matter

Masaki Asano^a, Kazuki Sakurai^{b,*}, Tsutomu T. Yanagida^c^a *Physikalisches Institut and Bethe Center for Theoretical Physics, Universität Bonn, Nussallee 12, D-53115 Bonn, Germany*^b *Department of Physics, King's College London, London WC2R 2LS, UK*^c *Kavli Institute for the Physics and Mathematics of the Universe (WPI), TODIAS, University of Tokyo, Kashiwa 277-8568, Japan*

ARTICLE INFO

Article history:

Received 29 May 2014

Received in revised form 22 July 2014

Accepted 24 July 2014

Available online 30 July 2014

Editor: J. Hisano

ABSTRACT

The gluino mass has been constrained by various search channels at the LHC experiments and the recent analyses are even sensitive to the cases where gluinos decay to quarks at the end of the decay chains through the baryonic RPV operator. We argue that introduction of extra matter, which is partly motivated by cancelling anomalies of discrete R symmetry, may help to relax the gluino mass limit when the RPV hadronic gluino decays are considered. In the scenarios where the extra matter states appear in the gluino decay chains, the number of decay products increases and each jet becomes soft, making it difficult to distinguish the signal from backgrounds. We investigate the sensitivity of existing analyses to such scenarios and demonstrate that the gluino mass limit can be relaxed if the mass spectrum reconciles the sensitivities of high p_T jet searches and large jet multiplicity searches.

© 2014 The Authors. Published by Elsevier B.V. This is an open access article under the CC BY license (<http://creativecommons.org/licenses/by/3.0/>). Funded by SCOAP³.

1. Introduction

The ATLAS and CMS Collaborations have conducted intensive and comprehensive searches for new physics during Run 1 of the LHC. To date, all searches have only found agreement between the Standard Model (SM) and data, which places stringent constraints on models beyond the SM (BSM). In particular, the R-parity conserved minimal supersymmetric SM (RPC MSSM) is severely constrained due to a lack of events in the large missing energy channels, and the gluino mass in RPC MSSM is constrained up to about 1 TeV [1,2].

The stringent limit on the gluino mass in the MSSM can be modified if R-parity violation (RPV) is introduced¹ [4–6]. In this case the LSP can decay promptly into visible particles, trading the large missing energy signature with large multiplicity of jets and leptons. The RPV scenario which is the most difficult to be searched for would be the one where the pair produced SUSY particles decay fully hadronically via the UDD baryonic RPV operator. Some of the recent ATLAS and CMS analyses however explicitly target such models and if the gluinos decay into three or five quarks, the six and seven jet analyses [7,8] exclude the gluinos lighter than 900 GeV.

In this paper we point out that the RPV scenario with extra matter may lead to event topologies where the gluino mass limit is more relaxed. The extra matter scenario is one of the interesting possibilities of the MSSM extensions. An advantage is that anomaly of discrete R-symmetry, Z_{NR} ($N > 2$), in the MSSM can be cancelled by the extra matter fields. For instance, it is known [9,10] that introduction of a $\mathbf{5} + \bar{\mathbf{5}}$ or a $\mathbf{10} + \bar{\mathbf{10}}$ chiral multiplet pair, or three pairs of $\mathbf{5} + \bar{\mathbf{5}}$ can achieve non-anomalous discrete R-symmetry. The discrete R-symmetry may play an important role in low-energy supersymmetry (SUSY) models. It controls dangerous proton decay operators as well as the constant term and supersymmetric μ term in the superpotential. The mass terms of extra matter states are also controlled by the discrete R-symmetry. For example, the mass terms with the similar scale to the soft SUSY breaking scale can be generated by the Giudice–Masiero mechanism [9–11].

If several extra matter states appear in the gluino decay chain, the number of final state particles becomes large and p_T of each visible particle tends to be small because the initial gluino mass energy is divided into a large number of decay products. The sensitivity of the current RPV SUSY searches then drops because of the high p_T jet requirement. The sensitivity of the existing analyses to the hadronically decaying gluinos with long cascade decay chains has been studied in Ref. [5]. The authors pointed out that the CMS black hole search [12] can effectively constrain the light gluinos in this scenario. We will demonstrate that the limit from

* Corresponding author.

¹ The gluino mass limit can also be relaxed in the models with compressed SUSY mass spectrum (see e.g. [3]).

the CMS black hole search can also be relaxed if there is a mild mass degeneracy between the gluino and the LSP.

The rest of the paper is organised as follows: the next section describes our model setup that includes extra matter and some RPV operators. In Section 3, we discuss the gluino decay chains in the RPV extra matter scenario. In Section 4, we reinterpret the existing analyses and study the gluino mass bound in the context of simplified models. Sections 5 and 6 are devoted to discussion and conclusion.

2. Extra matter with R-parity breaking operator

We consider models with extra $\mathbf{5} + \bar{\mathbf{5}}$ chiral multiplet pairs. We write $\mathbf{5}'_i = (D'_i, L'_i)$ and $\bar{\mathbf{5}}'_i = (\bar{D}'_i, \bar{L}'_i)$ and introduce the mass terms for these component fields.²

$$W \supset M_i^{L'} L'_i \bar{L}'_i + M_i^{D'} D'_i \bar{D}'_i, \quad (1)$$

where $M_i^{L'/D'} > M_j^{L'/D'}$ for $i < j$. In order to have multi-step hadronic gluino decays we introduce the RPV operators

$$W \supset \lambda_{212}' U_2 D_1 D_2 + \tilde{\lambda}_{1i}' L'_i Q_2 D_2 + \tilde{\lambda}_{iD}' D'_i D_2 U_2. \quad (2)$$

The first term is necessary to have the LSP decay into three light flavour quarks, whilst the second term is needed to make the gluinos decay to L'_i as well as to make L'_i decay to a lighter L'_j ($i < j$) or a neutralino lighter than L'_i as we will see in the next section. Similarly, the third term is introduced for the D' decay, although we assume that D' is heavier than the gluino and do not consider D' production for simplicity. Here and throughout the paper, L'_i and D'_i represent the superfields and/or fermionic components of the chiral multiplets and assume that the scalar components acquire the soft masses and are heavy enough not to contribute to our analysis.

Although the baryon number is violated by the UDD operator in our model, the lepton number is still conserved by declaring L' fields have zero lepton number. The proton decay constraint is thus avoided. To satisfy the constraint from $n-\bar{n}$ oscillation and suppress the single squark production we assume $\lambda_{212}'' \sim 10^{-3}$.

3. Gluino decay chain

In the models where the gluino is the LSP and the UDD operator is introduced, gluinos decay into three quarks: $\tilde{g} \rightarrow 3q$. If there is a neutralino below the gluino, the gluino can decay into five quarks through the neutralino: $\tilde{g} \rightarrow qq\tilde{\chi}_1^0 \rightarrow 5q$. For both cases, gluinos are severely constrained by the six and seven jet analyses [7,8] and the limit on the gluino mass is found at 900 GeV.

3.1. Gluino \rightarrow seven-quarks

If the fermionic component of $L' = (v', l')^T$ is lighter than the gluino, the gluinos can decay into two quarks and L' via off-shell squarks through the $L'_i Q_j D_k$ operator with the $\tilde{\lambda}_{ijk}'$ coupling. The L' can then decay into two quarks and a neutralino by the same mechanism as the gluino decay, $\tilde{g} \rightarrow qqL'$, if the neutralino is lighter than L' . The neutralinos finally decay into three quarks through the UDD operator. In this case the gluinos decay into seven quarks, $\tilde{g} \rightarrow qqL' \rightarrow qqqq\tilde{\chi}_1^0 \rightarrow 7q$, as shown in Fig. 1. Note that $\tilde{g} \rightarrow qq\tilde{\chi}_1^0$ is also kinematically allowed. However, $Br(\tilde{g} \rightarrow qqL')/Br(\tilde{g} \rightarrow qq\tilde{\chi}_1^0)$ is roughly, up to the phase space factor, proportional to $|\tilde{\lambda}_{ijk}'/g|^2$ with g being the electroweak gauge coupling

² We use a notation in which D , U and E represent the chiral multiplets containing anti-particles.

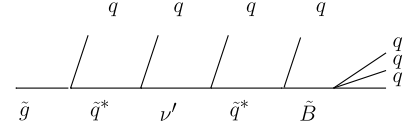


Fig. 1. Typical gluino decay chains which are induced by adding one pair of $\mathbf{5} + \bar{\mathbf{5}}$ extra matter multiplets with additional RPV terms.

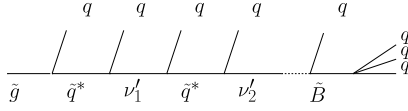


Fig. 2. Possible gluino decay chains which are induced by adding many extra matter with additional RPV term.

if the neutralino is gaugino-like. We therefore take $\tilde{\lambda}_{ijk}' \sim 1$ to suppress the $\tilde{g} \rightarrow qq\tilde{\chi}_1^0$ mode.

3.2. Gluino \rightarrow nine and more-quarks

If one introduces two or more $\mathbf{5} + \bar{\mathbf{5}}$ chiral multiplet pairs, even longer gluino decay chains are possible as shown in Fig. 2. To enhance the \tilde{g} and L' decay modes into the heaviest fermionic state possible, we assume a hierarchy in the couplings: $\tilde{\lambda}_{1jk}' > \dots > \tilde{\lambda}_{njk}' > g$.

As we have seen in this section, the RPV models with extra matter may lead to multi-step gluino decays producing a large number of quarks and no missing energy in the final state. In the next section, we reinterpret the existing analyses and study the gluino mass limit in the event topologies considered in this section.

4. The current LHC constraints

As discussed in the previous section, in the scenario where several extra matter states appear in the gluino decay chain and the LSP decays hadronically, the gluino may decay into fully hadronic final states without producing large missing energy. The event topology with such gluino decay chains is challenging to search for at the LHC for the following reasons: (1) standard SUSY searches that require large \cancel{E}_T are not sensitive to this topology. (2) The final state does not contain isolated leptons, which makes it difficult to distinguish the signal from the backgrounds with fully hadronic final states (e.g. QCD and fully hadronic $t\bar{t}$ + jets). (3) The gluino mass energy is divided into a large number of final state quarks, making each signal jet soft, which leads to degradation of signal efficiencies because of a high p_T cut threshold for the signal jets.

The sensitivity of the existing analyses to the models with hadronically decaying gluinos via the baryonic RPV operator has been studied in Ref. [5]. The authors pointed out that the most stringent constraints were obtained by the ATLAS 6–7 high p_T jet search [8] and the CMS black hole search [12]. The ATLAS 6–7 high p_T jet search looks for excesses in the 6 and 7 exclusive jet multiplicity bins with various p_T cuts: $> 80, 100, 120, 140$ and 180 GeV. The CMS black hole search, on the other hand, employs somewhat smaller p_T cut threshold, 50 GeV. The analysis uses a kinematic variable, S_T , which is defined as the scalar sum of all reconstructed objects, including \cancel{E}_T , with $p_T > 50$ GeV. Ref. [5] found that signal events may pollute the control region in the CMS black hole search and proposed a prescription which assumes the observed data is potentially entirely from signal, with zero background. This prescription provides conservative limits and we closely follow their analyses. In particular we use the signal regions ($S_T > 1.9$ and 2.2 TeV and $N_{obj} \geq 8, 9, 10$, where N_{obj} is the

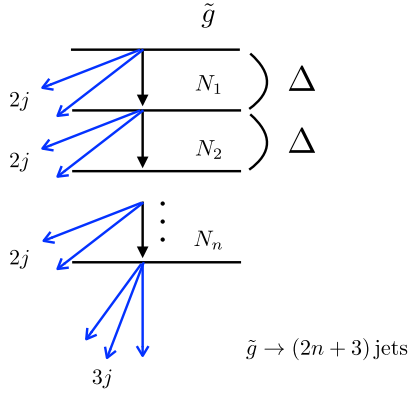


Fig. 3. A generalised gluino decay chain.

number of reconstructed objects, excluding \cancel{E}_T , with $p_T > 50$ GeV) and the corresponding visible cross section upper limits used in Ref. [5].

In order to estimate the gluino mass bound, we simulate events using Herwig++ [13]. Generated event samples are then passed to Delphes [14] to simulate detector responses, before estimating signal efficiencies for the signal regions. For the cross section of gluino pair production, we use the values reported by the LHC SUSY cross section working group [15], which includes NLO SUSY QCD corrections and the resummation of soft gluon emission at NLL accuracy.

To make complicated gluino decay chains tractable, we study the gluino mass limit following simplified model approach. In our analysis, we assume squarks are decoupled in the gluino decay and production process, and the gluino decay chain is generalised as a cascade decay through n intermediate BSM states, N_1, \dots, N_n , with each decay, except for N_n , producing two light flavour quarks, $\tilde{g} \rightarrow qqN_1, N_1 \rightarrow qqN_2, \dots, N_{n-1} \rightarrow qqN_n$, and N_n finally decays into three quarks via the UDD operator, $N_n \rightarrow qqq$. In this setup the gluinos decay into $(2n+3)$ light flavour quarks. In the extra matter scenarios, N s are either fermionic extra matter states or the MSSM neutralinos as discussed in the previous section. For simplicity we assume those BSM states (including gluino) have the same mass gap, Δ , namely $m_{\tilde{g}} - m_{N_1} = m_{N_1} - m_{N_2} = \dots = m_{N_{n-1}} - m_{N_n} \equiv \Delta$. Our generalised gluino decay chain is shown in Fig. 3.

Fig. 4 shows the ratio of the visible cross sections and the 95% CL upper limits for the 7 jet with $p_T > 180$ and 140 GeV signal regions by ATLAS (red solid and red dashed) and the 10 and 9 jet with $S_T > 2.2$ TeV signal regions by CMS (blue solid and blue dashed) as functions of the mass gap, Δ . The visible cross section is defined as $\sigma_{\text{vis}} = \sigma_{\tilde{g}\tilde{g}} \cdot \epsilon_i(\Delta)$, where $\sigma_{\tilde{g}\tilde{g}}$ is the gluino pair production cross section and $\epsilon_i(\Delta)$ is the efficiency for signal region i , which depends on the mass gap, Δ . The gluino mass is taken at 900 GeV and the upper and lower panels correspond to the models with $n = 2$ and 4, respectively. We have checked all the signal regions in the ATLAS 6–7 high p_T jet search [8] and the CMS black hole search [12] and found that those shown in Fig. 4 provide the strongest constraints.

As can be seen, the constraints obtained from the ATLAS high p_T jet search become weaker as the mass gap Δ increases up to 50–60 GeV. This is expected because the p_T scale of the jets coming from N_n decay is characterised by $m_{N_n} = m_{\tilde{g}} - n \cdot \Delta$. Conversely, the sensitivity of the CMS black hole search increases as Δ increases. This is because the search is sensitive to the events with large jet multiplicity, and the jets coming from the gluino and N_m ($m < n$) states become hard enough to pass the p_T cut in this analysis when Δ increases. Because of the above two effects, a window of the allowed region opens for the 900 GeV gluino

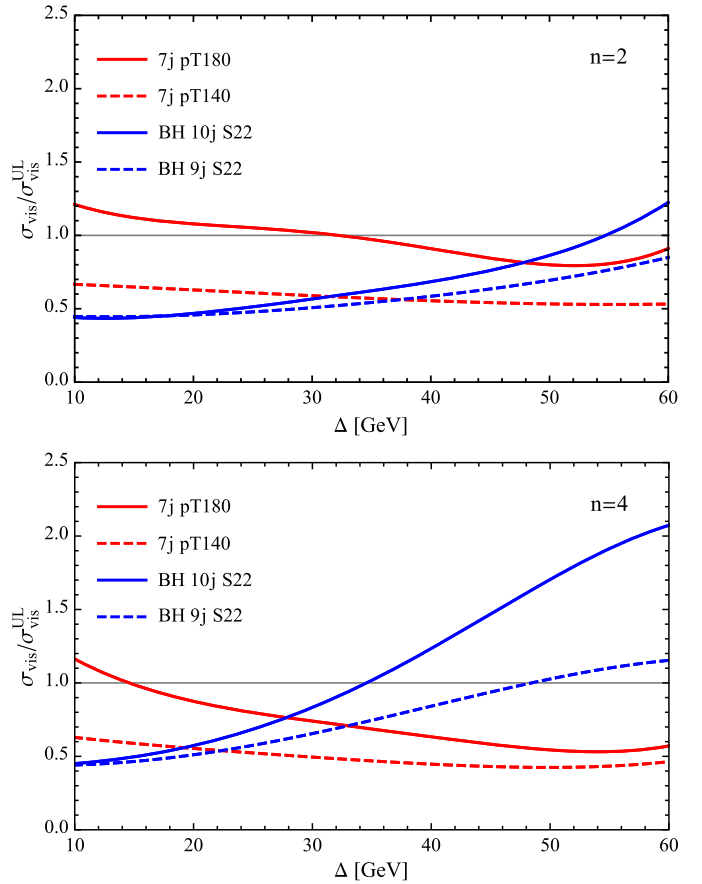


Fig. 4. The ratio of the visible cross sections and the 95% CL upper limits for the 7 jet with $p_T > 180$ and 140 GeV signal regions by ATLAS (red solid and red dashed) and the 10 and 9 jet with $S_T > 2.2$ TeV signal regions by CMS (blue solid and blue dashed) as functions of the mass gap, Δ . The gluino mass is taken at 900 GeV. The upper and lower panels correspond to the models with $n = 2$ and 4, respectively. (For interpretation of the references to colour in this figure legend, the reader is referred to the web version of this Letter.)

at some value of Δ . For the $n = 2$ model, this window appears in the $35 < \Delta/\text{GeV} < 55$ region. For the $n = 4$ model, these effects are more dramatic compared to the $n = 2$ case. Namely, the ATLAS constraints become weaker and the CMS constraints grows stronger more quickly when increasing Δ compared to the $n = 2$ case. Consequently, the allowed window for the $n = 4$ model appears in the more degenerate mass region: $15 < \Delta/\text{GeV} < 35$.

In realistic models, gluinos may have several possible decay modes. The branching ratio of each decay mode depends on the details of the model (the couplings and the mass spectrum). An exhaustive study of the LHC sensitivity allowing multiple gluino decay modes is beyond the scope of this paper. We, however, show the LHC sensitivity for a specific case to see how large the impact of the multiple gluino decay modes is. In Fig. 5, we show the normalised visible cross sections as a function of Δ for the $n = 2$ case as in the upper panel in Fig. 4 but allowing the two gluino decay modes: $\tilde{g} \rightarrow 2qN_2 \rightarrow 5q$ and $\tilde{g} \rightarrow 2qN_1 \rightarrow 4qN_2 \rightarrow 7q$ with the branching ratios of 30 and 70%, respectively. As can be seen, at the vicinity of the allowed region ($\sigma_{\text{vis}}/\sigma_{\text{vis}}^{\text{UL}} \leq 1$), the sensitivity is slightly increased compared to the $BR(\tilde{g} \rightarrow 7q) = 1$ case shown in the upper panel in Fig. 4. However, the sizable region of Δ still evades exclusion. We therefore expect that including the other gluino decay modes do not change our picture much as long as the simplified model decay chain dominates in the gluino decay modes.

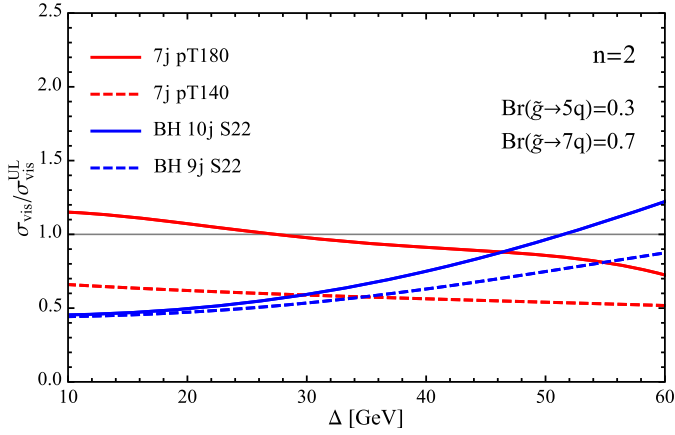


Fig. 5. The same plot as in the upper panel in Fig. 4, but the gluinos have two decay modes: $\tilde{g} \rightarrow 2qN_2 \rightarrow 5q$ and $\tilde{g} \rightarrow 2qN_1 \rightarrow 4qN_2 \rightarrow 7q$, where the branching ratios are assumed to be 30 and 70%, respectively.

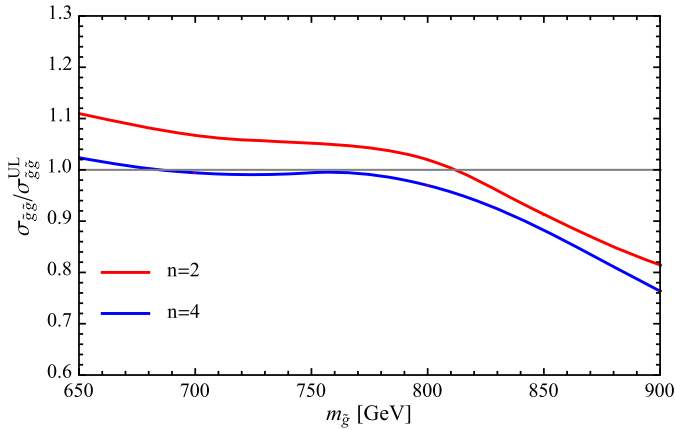


Fig. 6. Production cross section constraints for gluino.

In Fig. 6 we show the ratio of the gluino cross section and its 95% CL upper limit as a function of the gluino mass. Here we scan Δ for each gluino mass and choose the value which gives the weakest sensitivity for that gluino mass. We see that the gluino mass limit can be relaxed up to about 810 (680–780) GeV for the $n = 2$ (4) model.

5. Discussion

In the previous section, we found that in the $n = 2$ (4) model the ATLAS 6–7 jet analysis excludes a 900 GeV gluino only for the $\Delta < 30$ (15) GeV region, whilst the CMS black hole analysis does so only for the $\Delta > 55$ (35) GeV region. Consequently a gap in sensitivity arises at the 30 (15) $< \Delta/\text{GeV} < 55$ (35) region for the 900 GeV gluino in the $n = 2$ (4) model.

One can expect that this gap can be filled by introducing new signal regions which covers the intermediate region between the ATLAS 6–7 jet analysis and the CMS black hole analysis. Such new signal regions are shown as the green region in Fig. 7, where we summarise the current situation of the analyses by a schematic coverage table.

We would like to comment on the $n \gg 1$ limit. In this limit the gluino mass energy is divided into a very large number of quarks and p_T of each jet would become very small. Most of the quark jets would fail to pass the 50 GeV jet p_T cut and the analyses with such a p_T cut would not be effective to constrain the model. To search for $n \gg 1$ scenarios, one would need to extend the search

		jet p_T cut threshold (in GeV)						
		...	> 40	> 50	> 80	> 100	...	> 180
jet multiplicity bin	7			CMS BH search	ATLAS high p_T jet search			
	8							
	9							
	10							
	11							
	...							

Fig. 7. A schematic table for coverage.

region in the space of the jet p_T cut threshold and the jet multiplicity bin, as shown in the grey region in Fig. 7. In this region one has to look at either a very small jet p_T bin or a very large jet multiplicity bin. It is however challenging to accurately estimate the background contribution to such soft or large jet multiplicity bins.

We also comment on the CMS gluino resonance search [7]. This analysis looks for a bump in the three jet invariant mass distribution assuming $\tilde{g} \rightarrow qq\bar{q}$ topology using 19.5 fb^{-1} of pp collision data at $\sqrt{s} = 8 \text{ TeV}$. Although this is another constraint, we do not expect this analysis changes our result drastically. In the $n = 2$ and 4 models, gluinos decay into 7 and 11 quarks and three quark invariant mass does not reconstruct the gluino mass. Moreover, because of the large jet multiplicity, the combinatorial background is much larger in the $n = 2$ and 4 models, which would degrade the sensitivity of the analysis significantly.

The multi-step gluino decay chains can also be realised with the D' intermediate states. In this case the gluino mass bound would become stronger since D' production events would also contribute to the signal region. However, in the small Δ region, the production cross section of D' is smaller than that for the gluinos due to its smaller colour factor. The efficiency of the D' production events is also smaller since D' decays fewer quarks compared to the gluinos. We therefore expect that the gluino mass bound would not change drastically in the models with the D' intermediate states. If L' are also included in this system with $m_{\tilde{g}} > m_{D'} > m_{L'}$, the gluino decay chain would become longer and it may be helpful to relax the gluino mass bound.

We also comment on the models with a $10 + \overline{10}$ pair, where $10 = (Q', U', E')$ and $\overline{10} = (\overline{Q}', \overline{U}', \overline{E}')$. The multi-step gluino decay chains via the U' intermediate states are possible in this model using the $U'DD$ operator. Finally, it is worth pointing out that in our scenario the mass bound on the extra matter are also relaxed since the extra matter states decay fully hadronically through long cascade decay chains.

6. Conclusions

In this paper we pointed out that the RPV models with extra matter may lead to multi-step gluino decays into fully hadronic final states. We reinterpreted the existing analyses and studied the gluino mass bound in our generalised model. In the region where the mass gap Δ is small, the sensitivity of ATLAS 6–7 jets analysis decreases, whilst that of CMS black hole search increases as increasing Δ . Consequently, the current LHC sensitivity is minimised at some value of Δ . In the simulation we demonstrated that the gluino mass bound in such scenarios can be as small as 700 or 800 GeV depending on the number of intermediate states in the gluino decay chain.

In order to increase the sensitivity to the gluinos that undergo multi-step cascade decays into fully hadronic final states, it is important to extend the search strategy in the space of the jet p_T cut threshold and the jet multiplicity bin, which requires a better understanding of the backgrounds contributing the soft and large jet multiplicity bins.

Acknowledgements

M.A. acknowledges support from the German Research Foundation (DFG) through grant BR 3954/1-1 and DFG TRR33 “The Dark Universe”. The work of K.S. was supported in part by the London Centre for Terauniverse Studies (LCTS), using funding from the European Research Council via the Advanced Investigator Grant 267352. The work of T.T.Y. was supported by Scientific Research (B) No. 26287039 [T.T.Y.] and World Premier International Center Initiative (WPI Program), MEXT, Japan.

References

- [1] ATLAS Collaboration, ATLAS-CONF-2013-047.
- [2] S. Chatrchyan, et al., CMS Collaboration, arXiv:1402.4770 [hep-ex].
- [3] J. Alwall, M.-P. Le, M. Lisanti, J.G. Wacker, Phys. Lett. B 666 (2008) 34, arXiv:0803.0019 [hep-ph];
E. Izaguirre, M. Manhart, J.G. Wacker, J. High Energy Phys. 1012 (2010) 030, arXiv:1003.3886 [hep-ph];
T.J. LeCompte, S.P. Martin, Phys. Rev. D 84 (2011) 015004, arXiv:1105.4304 [hep-ph];
T.J. LeCompte, S.P. Martin, Phys. Rev. D 85 (2012) 035023, arXiv:1111.6897 [hep-ph];
H. Murayama, Y. Nomura, S. Shirai, K. Tobioka, Phys. Rev. D 86 (2012) 115014, arXiv:1206.4993 [hep-ph];
K. Rolbiecki, K. Sakurai, J. High Energy Phys. 1210 (2012) 071, arXiv:1206.6767 [hep-ph];
H.K. Dreiner, M. Kramer, J. Tattersall, Europhys. Lett. 99 (2012) 61001, arXiv:1207.1613 [hep-ph];
B. Bhattacharjee, K. Ghosh, arXiv:1207.6289 [hep-ph];
S. Mukhopadhyay, M.M. Nojiri, T.T. Yanagida, arXiv:1403.6028 [hep-ph].
- [4] B.C. Allanach, B. Gripaios, J. High Energy Phys. 1205 (2012) 062, arXiv:1202.6616 [hep-ph];
M. Asano, K. Rolbiecki, K. Sakurai, J. High Energy Phys. 1301 (2013) 128, arXiv:1209.5778 [hep-ph];
J.A. Evans, Y. Kats, J. High Energy Phys. 1304 (2013) 028, arXiv:1209.0764 [hep-ph];
D. Curtin, R. Essig, B. Shuve, Phys. Rev. D 88 (2013) 034019, arXiv:1210.5523 [hep-ph];
Z. Han, A. Katz, M. Son, B. Tweedie, Phys. Rev. D 87 (2013) 075003, arXiv:1211.4025 [hep-ph];
T. Cohen, E. Izaguirre, M. Lisanti, H.K. Lou, J. High Energy Phys. 1303 (2013) 161, arXiv:1212.1456 [hep-ph];
B. Bhattacharjee, J.L. Evans, M. Ibe, S. Matsumoto, T.T. Yanagida, Phys. Rev. D 87 (2013) 115002, arXiv:1301.2336 [hep-ph];
B. Bhattacharjee, A. Chakraborty, arXiv:1311.5785 [hep-ph];
P. Graham, S. Rajendran, P. Saraswat, arXiv:1403.7197 [hep-ph].
- [5] J.A. Evans, Y. Kats, D. Shih, M.J. Strassler, arXiv:1310.5758 [hep-ph].
- [6] For recent theoretical studies, e.g., E. Nikolidakis, C. Smith, Phys. Rev. D 77 (2008) 015021, arXiv:0710.3129 [hep-ph];
C. Csaki, Y. Grossman, B. Heidenreich, Phys. Rev. D 85 (2012) 095009, arXiv:1111.1239 [hep-ph];
J.T. Ruderman, T.R. Slatyer, N. Weiner, J. High Energy Phys. 1309 (2013) 094, arXiv:1207.5787 [hep-ph];
G. Krnjaic, D. Stolarski, J. High Energy Phys. 1304 (2013) 064, arXiv:1212.4860 [hep-ph];
R. Franceschini, R.N. Mohapatra, J. High Energy Phys. 1304 (2013) 098, arXiv:1301.3637 [hep-ph];
C. Csaki, B. Heidenreich, Phys. Rev. D 88 (2013) 055023, arXiv:1302.0004 [hep-ph];
A. Florez, D. Restrepo, M. Velasquez, O. Zapata, Phys. Rev. D 87 (2013) 095010, arXiv:1303.0278 [hep-ph];
G. Krnjaic, Y. Tsai, J. High Energy Phys. 1403 (2014) 104, arXiv:1304.7004 [hep-ph];
A. Montoux, Phys. Rev. D 88 (2013) 045029, arXiv:1305.2921 [hep-ph];
L. Di Luzio, M. Nardecchia, A. Romanino, Phys. Rev. D 88 (2013) 115008, arXiv:1305.7034 [hep-ph];
A. Arvanitaki, M. Baryakhtar, X. Huang, K. van Tilburg, G. Villadoro, J. High Energy Phys. 1403 (2014) 022, arXiv:1309.3568 [hep-ph];
C. Csaki, E. Kuflik, T. Volansky, Phys. Rev. Lett. 112 (2014) 131801, arXiv:1309.5957 [hep-ph];
J. Bernon, C. Smith, arXiv:1404.5496 [hep-ph].
- [7] CMS Collaboration, CMS-PAS-EXO-12-049.
- [8] ATLAS Collaboration, ATLAS-CONF-2013-091.
- [9] K. Kurosawa, N. Maru, T. Yanagida, Phys. Lett. B 512 (2001) 203, arXiv:hep-ph/0105136.
- [10] M. Asano, T. Moroi, R. Sato, T.T. Yanagida, Phys. Lett. B 705 (2011) 337, arXiv:1108.2402 [hep-ph].
- [11] G.F. Giudice, A. Masiero, Phys. Lett. B 206 (1988) 480.
- [12] S. Chatrchyan, et al., CMS Collaboration, J. High Energy Phys. 1307 (2013) 178, arXiv:1303.5338 [hep-ex].
- [13] M. Bahr, S. Gieseke, M.A. Gigg, D. Grellscheid, K. Hamilton, O. Latunde-Dada, S. Platzer, P. Richardson, et al., Eur. Phys. J. C 58 (2008) 639, arXiv:0803.0883 [hep-ph];
K. Arnold, L. d'Errico, S. Gieseke, D. Grellscheid, K. Hamilton, A. Papaefstathiou, S. Platzer, P. Richardson, et al., arXiv:1205.4902 [hep-ph];
J. Bellm, S. Gieseke, D. Grellscheid, A. Papaefstathiou, S. Platzer, P. Richardson, C. Rohr, T. Schuh, et al., arXiv:1310.6877 [hep-ph].
- [14] J. de Favereau, et al., DELPHES 3 Collaboration, J. High Energy Phys. 1402 (2014) 057, arXiv:1307.6346 [hep-ex].
- [15] <https://twiki.cern.ch/twiki/bin/view/LHCPhysics/SUSYCrossSections>;
See also, http://pauli.uni-muenster.de/~akule_01/nllwiki/index.php/NLL-fast.